Peer-reviewed version available at Energies 2018, 11, 2953; doi:10.3390/en11112953

Article

A New ANFIS-based Peak Power Curtailment in Microgrids including PV Units and BESSs

Srete Nikolovski[1], Hamid Reza Baghaee[2] and Dragan Mlakić[3]

[1] Power Engineering Department, Faculty of Electrical Engineering, Computer science and Information Technology, University of Osijek, Osijek, Croatia: srete.nikolovski@ferit.hr ;
[2] Department of Electrical Engineering, Amirkabir University of Technology, Tehran, Iran hrbaghaee@aut.ac.ir,
[3] Department of Measurement and Network Management in Electrical Energy Systems, Distribution Area, Centar", JP Elektroprivreda HZ HB" d.d, Mostar, Mostar, Bosnia and Herzegovina; dragan.mlakic@ephzhb.ba

Abstract: One of the most crucial and economically beneficial tasks for energy customer is peak load curtailment. On account of the fast response of renewable energy resources (RERs) such as photovoltaic (PV) units and battery energy storage system (BESS), this task is closer to be efficiently implemented. Depends on the customer peak load demand and energy characteristics, the feasibility of this strategy may warry. When adaptive neuro-fuzzy inference system (ANFIS) is exploited for forecasting, it can provide many benefits to address the above-mentioned issues and facilitate its easy implementation, with short calculating time and re-trainability. This paper introduces a data driven forecasting method based on fuzzy logic for optimized peak load reduction. First, the amount of energy generated by PV is forecasted using ANFIS which conducts output trend, and then, the BESS capacity is calculated according to the forecasted results. The trend of the load power is then decomposed in Cartesian plane into two parts, left and right from load peak, searching for BESS capacity equal. Network switching sequence over consumption is provided by a fuzzy logic controller (FLC) with respect to BESS capacity and PV energy output. Finally, to prove the effectiveness of the proposed ANFIS-based peak shaving method, offline digital time-domain simulations have been performed on a real-life practical test micro grid system in MATLAB/Simulink environment and the results have been experimentally verified by testing on a practical micro grid system with real-life data obtained from smart meter and also, compared with several previously-reported methods.

Keywords: Adaptive neuro-fuzzy inference system, battery energy storage, photovoltaic unit, power demand, peak power curtailment.

1. Introduction

The concept of smart micro grids has emerged from high penetration of distributed generation (DG) and distributed /renewable energy resources (DERs/RERs) and energy storage systems (ESS) [1]-[3]. A micro grid is a small-scale, low-voltage power grid in the low voltage designed to solve energy issues locally and enhance flexibility. These systems can function in either grid-connected or islanded (autonomous) modes of operation [4]-[6]. The growth trend of RERs and constant power cost rise, brings new dimension of old problems exposing new ways. RERs, DERs and ESSs forces distribution network (DN) to be more flexible, faster, safer, and less expensive [7]-[9]. On the other hand, customer of distribution system operator (DSO) tends to use all capabilities of RERs/DERs provides with minimum human involvement [10]. Power peak curtailment is an old problem with new possible solutions. Micro and smart grids tend to provide new algorithms for power peak curtailment such as game theory in role of locating and displacing load in DN [11]. Some researchers have been conducted for integration of DERs into DN based on optimization tools and dynamic programming methods [12]. Demand side management of DNs, especially in micro and smart grid applications, also need new materials for energy efficiency [13]..

In addition, many new trends tend to increase load peak power on DN based o battery charging of plugged in hybrid electric vehicles (PHEVs) in charging stations [14]-[15]. Peak shaving with DERs/RERs and BESS are one of the major issues in micro grid power management. Role of ESS in peak shaving of medium voltage direct current (MVDC) systems based on smart algorithms has been discussed [16]. Forecasting power demand or energy consumption is also essential which has been done before based on fuzzy logic, artificial neural networks (ANNs) and particle swarm optimization (PSO) [17]-[18]. Fuzzy logic has been also used to manage available energy sources for peak power curtailment in a system composed of RERs and/or energy accumulations [19]-[20].

In this paper, a new method for load peak curtailment/shaving is proposed by combining essential components for optimizing peak power curtailment. This paper combines DERs/RERs with BESS connected to customer and microgrid that have been modeled and simulated in MATLAB/ Simulink software environment and then, experimentally tested on a practical test system. The proposed solution includes three parts: 1) Describing the proposed system configuration based on real-life existing examples in DSO networks 2) Presenting the proposed methodology based on ANFIS to forecast energy generation and power-peak demand with dimensioned energy components of the system configuration and, 3) Exploiting fuzzy logic controller (FLC) as major part to determine optimal BESS usage for the sake of power peak curtailment. Finally, to show the effectiveness of the proposed method, offline digital time-domain simulation studies are performed in MATLAB/ Simulink environment and after comparing the results with previously-reported methods, they are experimentally verified by testing on a practical micro grid system with real-life data obtained from smart meter.

The paper covers mentioned themes as follows: Section IV describes the system configuration. Section V elaborates on the proposed peak shaving method. Section IV presents the ANFIS and its structure for forecasting application. Section V presents simulation results. Finally, conclusions and final remarks are provided in Section VI to summarize all points.

2. System Configuration

As illustrated in Figure.1, the micro grid system mainly consists of: 1) DERs//RERs and ESSs, 2) DN and, 3) Customer of electric energy with various energy consumers.

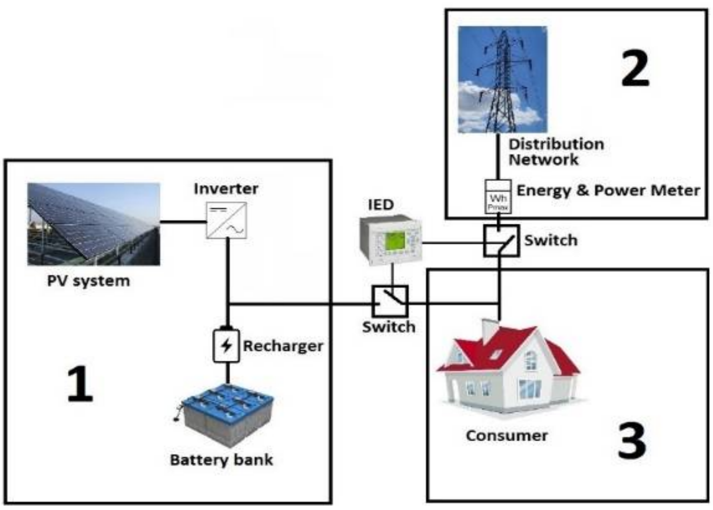

Figure. 1. Microgrid system configuration.

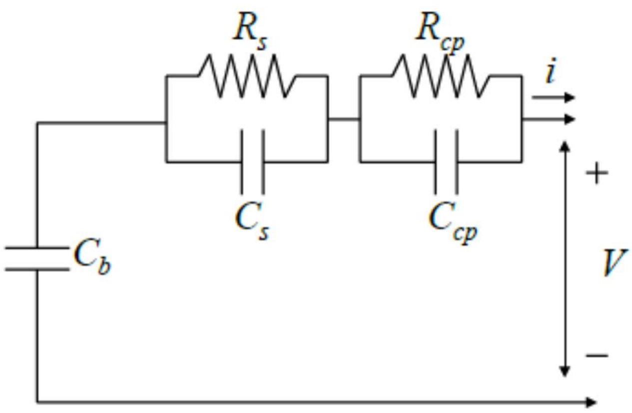

Figure. 2. Equivalent battery cell scheme for modeling BESS [21].

The goal of this study is: 1) minimize or ideally, deduct maximum power demand from customer's electricity bill, and 2) Independent focusing of energy for power peak demand curtailment, considering other related technical issues. In this study, DER/ RER is assumed to be a photovoltaic (PV) unit; however, this study can be performed based on any other type of DERs/RERs such as wind generation, thermal energy source, hydro plant, etc. There is the same situation for ESS, but the purpose of this paper is focused on BESS in role of ESS. The PV and BESS are installed on same site to give minimal or no voltage drop, and both are dimensioned as:

$$C_b = \sum_{h=0}^{24} E_{Pt}(h) \tag{1}$$

When BESS is considered as ESS, the most important issue is state of charge (SoC). The BESS can be modeled according to Figure.2 for one battery cell [21]. BESS is a string of single batteries that are unified as one battery cell. SoC is to be taken from BESS model as (Figure. 2) [21]:

$$\begin{aligned} C_b &= C_{Cbo} + C_{Cb1} \times SoC + C_{Cb2} \times SoC^2 \\ &+ \cdots + C_{Cbi} \times SoC^i \end{aligned} \tag{2}$$

$$C_b = C_{Cpo} + C_{Cp1} \times e^{(C_{Cp1} SoC)} + \cdots + C_{Cpi} \times e^{(C_{Cpi} SoC)} \tag{3}$$

where $i = 1, 2, \ldots, n$. For simpler presentation of BESS and its functionality in case study, C_s and R_s are taken minimal so impact of snubbed resistance of battery is high enough and battery engagement is fast enough. So, the *SoC* is defined as follows:

$$SoC = 1 - \frac{q_{\max} - q_b}{C_{\max}} \tag{4}$$

For effective management of BESS, SoC is basically the only required information. However, for dimensioning of BESS and calculating its SoC, Cb is still required. BESS is assembled of batteries for gathering energy capacity large enough for daily PV generation on sunny days (Figure.3). In this way, BESS will always be able to gather all generated electric energy and use it for over peak curtailment. PV is modeled based on available sun irradiance at installation site and power load peak demand based on smart meter data gathered from monthly readout. The PV output power is given by [22]:

Preprints (www.preprints.org) | NOT PEER-REVIEWED | Posted: 30 September 2018 doi:10.20944/preprints201809.0594.v1

Peer-reviewed version available at Energies 2018, 11, 2953; doi:10.3390/en11112953

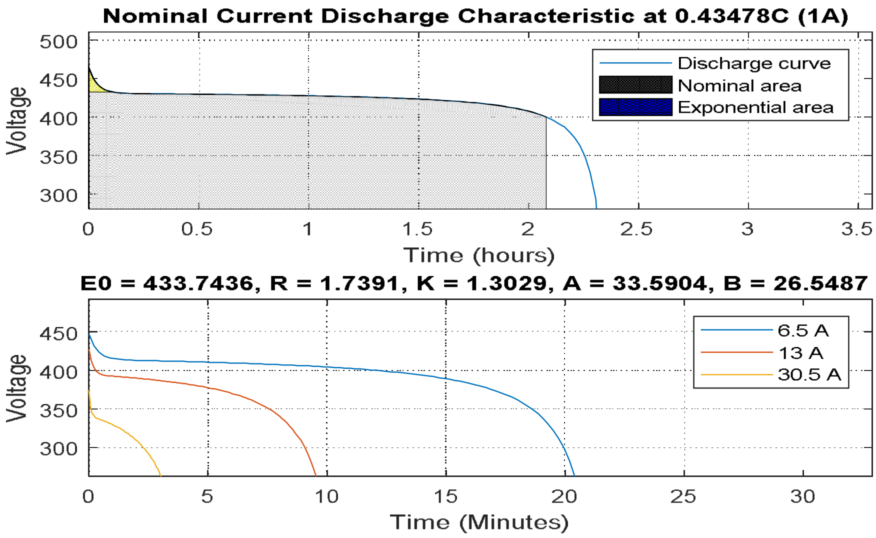

Figure. 3. SoC curve of BESS assembled used in case study.

$$P_t = C\frac{P_{PV,t}}{1000}\left[1-\mu\left(T_{PV,t}-25\right)\right] \tag{5}$$

Considering that C and μ are constant factors in (5), we conclude that P_t can be forecasted based only on $I_{PV,t}$ and $T_{PV,t}$. Figure.4 illustrates *I-V* and *P-V* characteristic from designed PV for case study simulations. The DN is modeled as infinite bus that consists of infinite power and ESSs are ready for customer engagement at any time. Just like in real-life practical case, DN is always on and ready for usage from customer. In this paper, internal resistance of grid model is considered to be near zero so that this relation is focused: PV + BESS → Customer ↔ DN. Also, the customer is modeled as one 10 kW power demand. Various power consumers inside customer's house hold are presented by daily power demand curve presented in Figure. 5 whose data has been gathered from energy and power meter between DN and customer. The placement of smart meter is presented on Figure. 1. Sizing of PV and BESS has been done based on customer's power demand and energy consumption curve from Figure. 5.

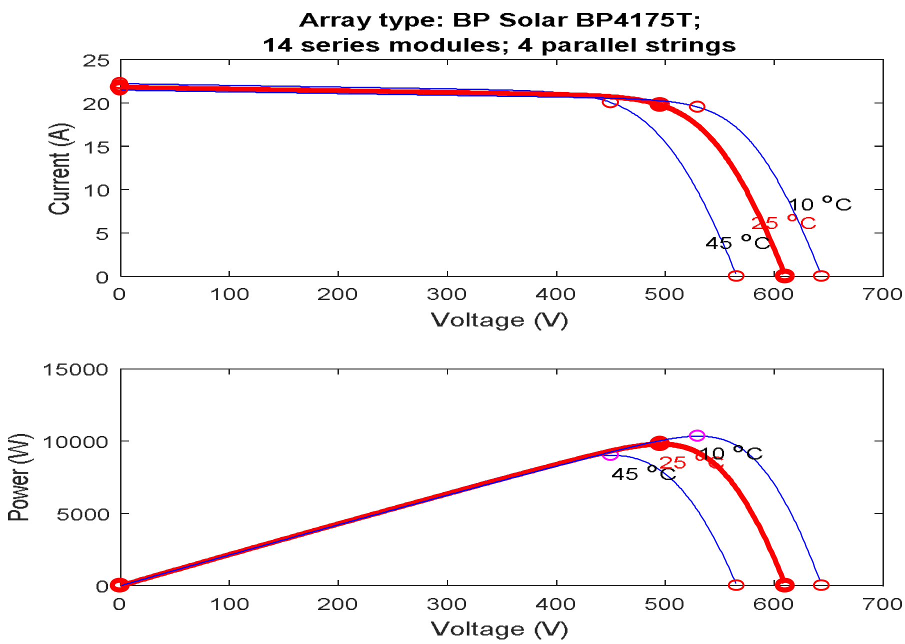

Figure. 4. PV *I-V* and *P-V* curve at 25°C and different sun irradiance.

Peer-reviewed version available at Energies 2018, 11, 2953; doi:10.3390/en11112953

Figure. 5. 10 kW customers daily power demand curve based on Smart Meter data.

However, in these cases, some optimal sizing algorithms are beneficial [23]-[26]. Based on the articles of the contract between DSO and customer, the maximum power reserved for customer is 10 kW namely we should have:

$$C = 10\,kW \tag{6}$$

where C can be much more or less; however, considering customers power peak, there is no need for over dimensioning RERs. There is the same story with BESS and C_b can be higher than C. The best guideline for dimensioning C_b is PV energy generation during the longest day of the year. According to customer's geographical location (Croatia, Zagreb), it is concluded that the longest day was 21.06.2017, with 15 hours and 36 minutes of sunlight and maximum temperature of 30 °C. Based on this information, DN operator`s database is searched for PV energy generation of 10 kW on that day and the output resulted from database is presented on Figure.6 that depicts PV generation curve on 21.6.2017. Basically, the PV can generate as much energy that BESS is be able to store. In reality, the longest day doesn't have to be necessarily the most productive day of PV, but it is good start for the first parameterization of PV capacity. Also in practice, a 10 kW customer rarely achieve higher power swell, but PV with 10 kWp installed capacity commonly achieve about 7 kW generated power peak. Owing to this fact, value of C in (6) is more than enough. Table 1 shows the days before and after the target day. Based on Figure.6 and Table 1, C_b should be 54 kWh. There are some more productive days for PV; but, there is no need for over dimensioning BESS. If the PV takes the maximum sun irradiation, the BESS is ready to accumulate entire energy generation from PV which results in $SoC \leq 100\%$. In this way, the PV never over recharge the BESS, and BESS make most of accumulated energy on power peak curtailment.

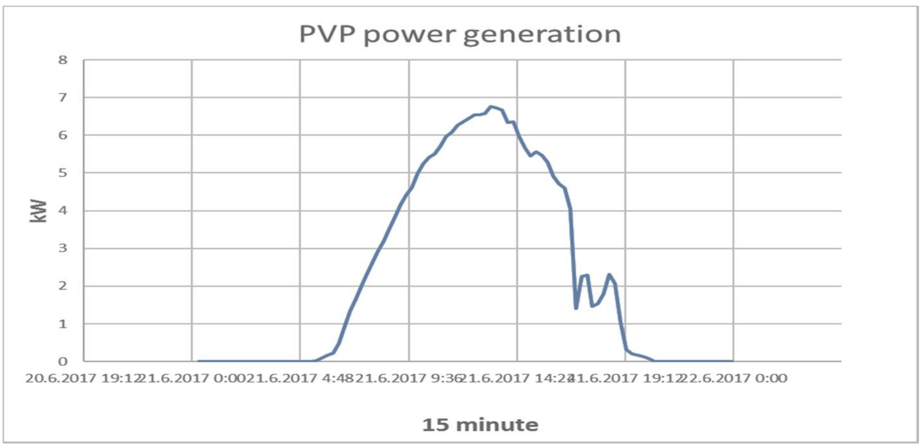

Figure. 6. 10 kW PV generation curve on longest day in year, 21.06.2017.

Peer-reviewed version available at Energies 2018, 11, 2953; doi:10.3390/en11112953

Table 1. Energy Generation of 10 Kw PV before and after longest day in year.

Day	Energy [kWh]
18.6.2017	19.12
19.6.2017	52.07
20.6.2017	58.31
21.6.2017	54.42
22.6.2017	54.59
23.6.2017	47.78
24.6.2017	53.54

3. Proposed Methodology

The proposed methodology for power peak demand reduction using ANFIS forecasting algorithm for estimation of energy generated by PV and BESS is illustrated in Figure. 7. The proposed power peak curtailment algorithm includes the following steps:

1) Calculating SoC of BESS based on PV output forecasted from daily input data, and forecasted customer`s daily consumption curve from which load peak is calculated,

2) Calculating the left and right energy consumption value from peak load with given parameters and calculation step, and summing both,

3) Comparing with BESS capacity based on *SoC*, if not equal, Jump to 2 and

4) Giving switch boundaries for training input for FLC.

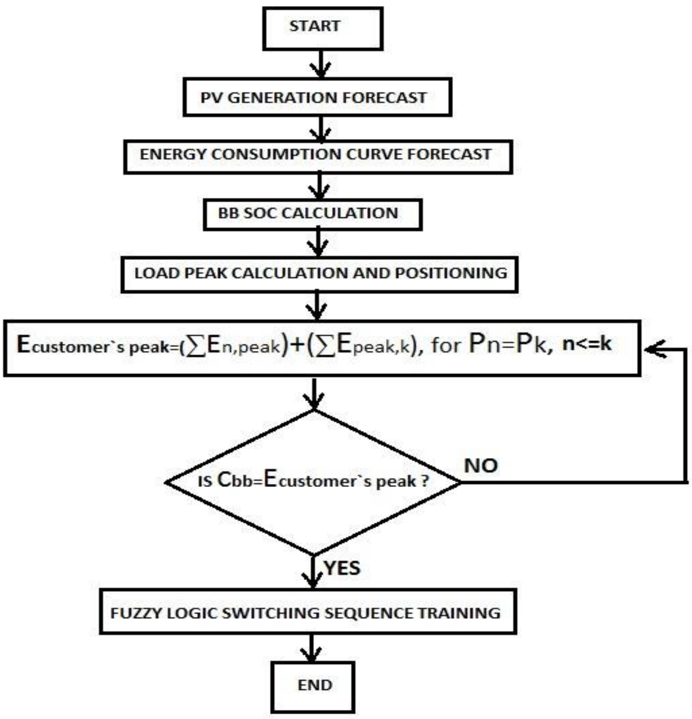

Figure. 7. Flowchart of the proposed algorithm.

Preprints (www.preprints.org) | NOT PEER-REVIEWED | Posted: 30 September 2018 doi:10.20944/preprints201809.0594.v1

Peer-reviewed version available at Energies 2018, 11, 2953; doi:10.3390/en11112953

In this paper, the ANFIS is used for forecasting of PV day ahead power generation. On account of its flexibility and processing speed, the ANFIS has been widely used as a method of forecasting method [17], [27]. The first stage of the algorithm is defining input and output datasets. In this study, the input data for PV generation forecasting are temperature, solar irradiance, and present day generation curve. According to (5), there is enough amount of input data to forecast day ahead. The most important part of data is present day generation curve because the first two inputs can be same in different parts of the year and instead of global, ANFIS may provide local solution. Combination of the mentioned three information is unique for any PV system. The second part of input data is the quality of information. Based on [17], [27], there is available daily temperature and sun irradiance but the resolution of these information should be discussed. For present day generation curve, one info per day is enough for temperature and irradiance just for 15-minute resolution. By using this method, the generalization of input data is avoided and therefore, mapping of input to output data is still achievable. The 15-minute resolution is based on smart meter recording upon which DSO charges customers to draw power peak. For the second input, the measurement unit is kWh/m2/day. Based on the amount of power radiated from sun, the PV is generating equivalent electricity power. This information is directly correlated if the PV module is stationary and with fixed latitude and array tilt. The sun irradiation is calculated based on (7)-(10).

$$Sunrise = 12 - \frac{1}{15^o}\left(\cos\left(\frac{-\sin(\varphi)\sin(\delta)}{\cos(\varphi)\cos(\delta)}\right)\right)^{-1} \tag{7}$$

$$Sunset = 12 + \frac{1}{15^o}\left(\cos\left(\frac{-\sin(\varphi)\sin(\delta)}{\cos(\varphi)\cos(\delta)}\right)\right)^{-1} \tag{8}$$

$$ID = 1.353 \times 0.7^{\left(AM^{0.678}\right)} \tag{9}$$

$$AM = 1/\cos(\theta) \tag{10}$$

Considering linear relationship between temperature, sun irradiance, and daily generation given in (5), the probabilistic curve forecasting method is capable to adapt the input data to output samples [27]. The PV generation curve in 15-minute resolution is acquired from data collecting software installed for supervision (Figure.6). The Energy consumption forecasting is solely based on temperature and the present day customer's consumption. The forecasting is left for ANFIS and according to our previous experiences, these inputs are temperature, and present day consumption curve. The present day consumption is acquired from smart meter installed between customer and DN (Figure.1). Based on the customer's agreement with DSO, the data access is available in 15-minute resolution. The basic idea behind step 3 is to convert the predicted peak load power curve from kW into kWh based on readout resolution and peak load point. The readout resolution is referenced to input data of peak load forecasting block, and its source is the smart meter between DN and customer (Figure. 1). Based on forecasted load peak, the graphical representation for calculation of customer's peak energy is shown in Figure. 8.

Preprints (www.preprints.org) | NOT PEER-REVIEWED | Posted: 30 September 2018 doi:10.20944/preprints201809.0594.v1
Peer-reviewed version available at Energies 2018, 11, 2953; doi:10.3390/en11112953

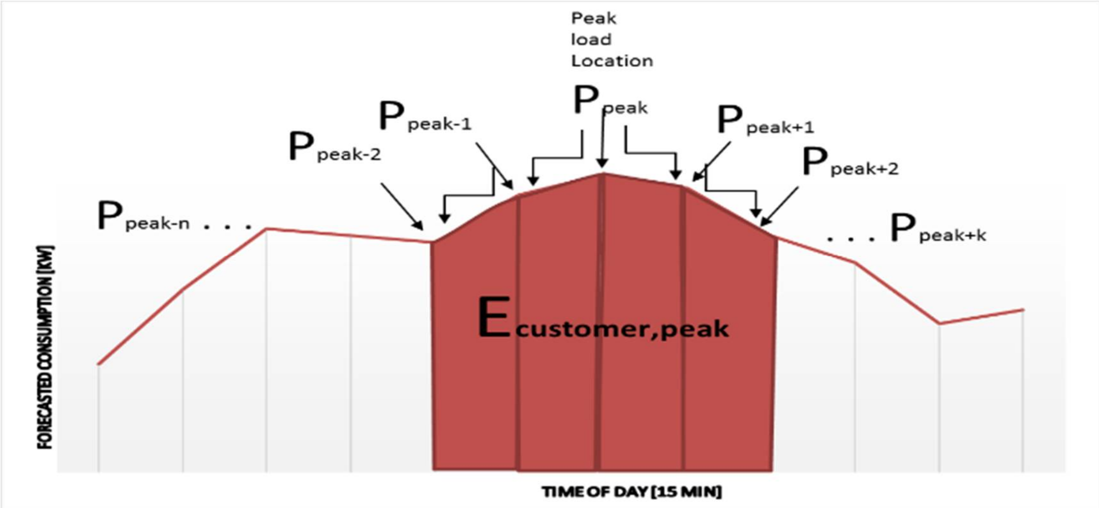

Figure. 8. Calculation of customer's energy around load peak by adding energy left and right from load peak location.

Also, we have:

$$E_{customer,peak} = \sum_{0}^{peak} E_{peak} + \sum_{peak}^{96} E_{peak+k};\ n < k \tag{11}$$

$$E_{peak-n} = E_{peak-n} \times 1/4 \tag{12}$$

$$E_{peak+k} = E_{peak+k} \times 1/4 \tag{13}$$

Table 2. The Training Parameters of ANFIS.

Parameter	Value (Case 1)	Value (Case 1)
Number of nodes	23	38
Number of linear parameters	9	16
Number of nonlinear parameters	12	24
Number of training data pairs	2784	2784
Number of fuzzy rules	3	4

Preprints (www.preprints.org) | NOT PEER-REVIEWED | Posted: 30 September 2018 doi:10.20944/preprints201809.0594.v1

Peer-reviewed version available at Energies 2018, 11, 2953; doi:10.3390/en11112953

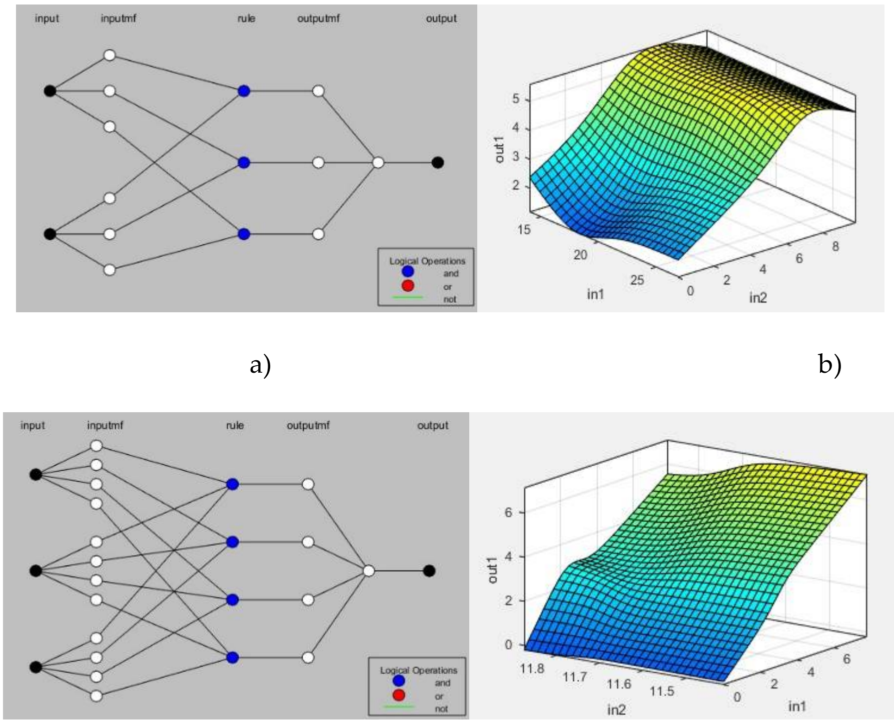

a) b)

b) d)

Figure 10. a) ANFIS forecast system architecture for power load forecast. B) Surface for ANFIS`s 2 inputs and 1 output, c) ANFIS forecast system architecture for power generation forecast, b) Surface for ANFIS`s 3 inputs and 1 output.

Expression (11) models the process step 3 with time resolution of 15-minute and (12) and (13) give the energy calculation based on peak load at the given time. The steps n and k are 15-minute step left and right from peak location on timeline. One iteration is (11) for every n-1, k+1 and each iteration is subjected to this question that is the Cb equal to $E_{customer}$, peak? If yes, then the boundaries of switching sequence changes are given as P_{peak-n}, and P_{peak+k}. Basically, as soon as the smart meter records P_{peak-n}, the IED closes the switch between PV+BESS and customer and opens the switch between DN and customer. This switch state gives no power and energy to the smart meter to record because entire consumption is loaded on BESS. In this situation, the PV is still working as recharging source for BESS, the SoC is at the calculated state, and the BESS is energy source until the IED changes the switching state back at P_{peak+k}. even if $SoC > 0\%$. So, the BESS is not fully discharged and load peak is not recorded by DSO smart meter. P_{peak-n}, and P_{peak+k} are two MFs to FLC in role of IEDs. Using FL, as switching driving method, it may initiate switching at local load peak and not at global during real time recording. As can be observed from Figure. 9, there is a noticeable trend for localized peaks and for global peaks. Many local peaks happen during the day, but the global maximum is around samples 30-50 along with 70-85. This makes one more input to FLC switching algorithm with 2 membership functions (MFs). The Input of the sample number is usable if and only if the FLC knows which season of the year currently is: winter, spring, summer, or autumn. The need for these information comes from different possible global maximum (Figure. 8).

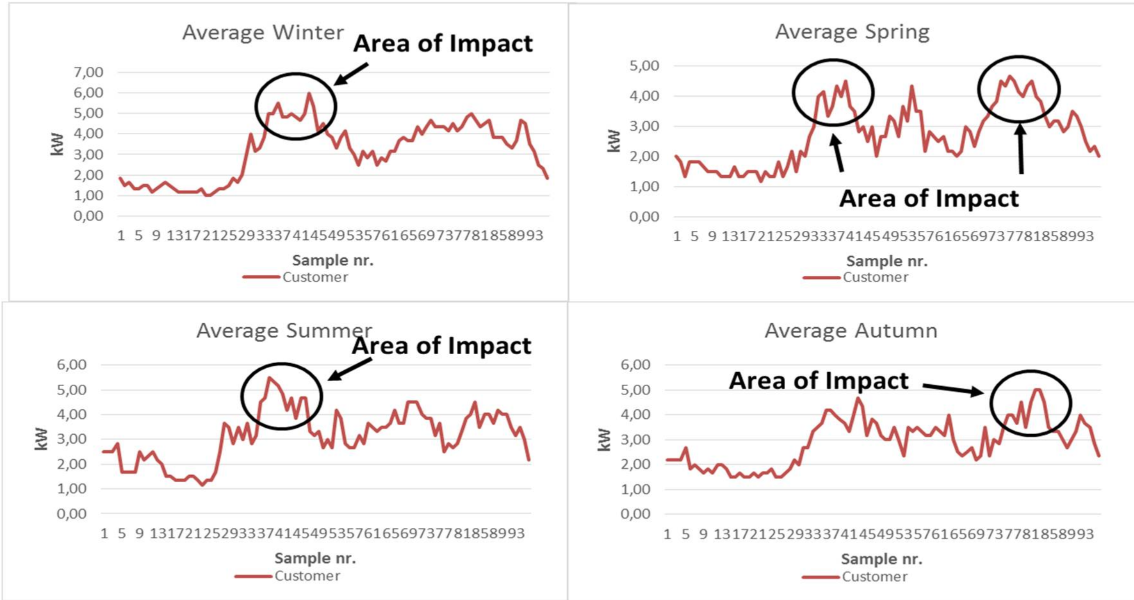

Figure. 9. Average load curve for all four seasons.

The global maximum location is located in the first MF for winter and summer, and the second MF for spring and autumn. This issue makes one additional input for FL switching algorithm with two MFs: one for winter and summer, and the second one for spring and autumn. The input values are left for forecasting the specific day load curve and therefore training of FLC. The fuzzy sets are defined by MF and rules so that the crisp values are processed into fuzzy values and then deffuzified. In this paper, triangular and trapezoid MFs are exploited. If there is a huge error in the output, is Gaussian-Triangular trapezoid MFs can be used. In this application, the output error is in acceptable range. The FLC have 3 inputs and 1 output whose MFs are defined as follows:

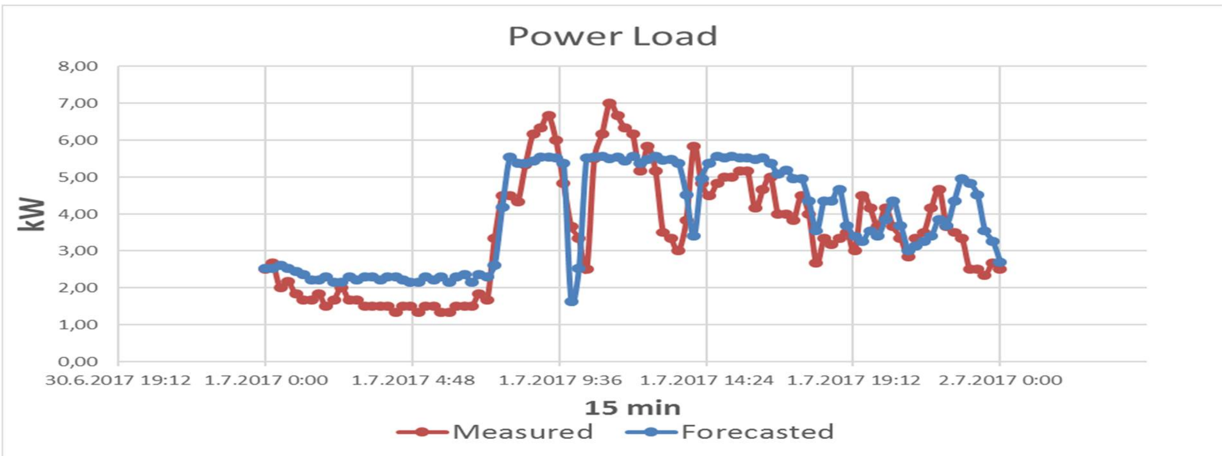

Figure. 11. Example customer (10 kW) forecasted for 1 day ahead compared with measured data from Smart Meter. Red: measured, blue: forecasted.

Preprints (www.preprints.org) | NOT PEER-REVIEWED | Posted: 30 September 2018 doi:10.20944/preprints201809.0594.v1

Peer-reviewed version available at Energies 2018, 11, 2953; doi:10.3390/en11112953

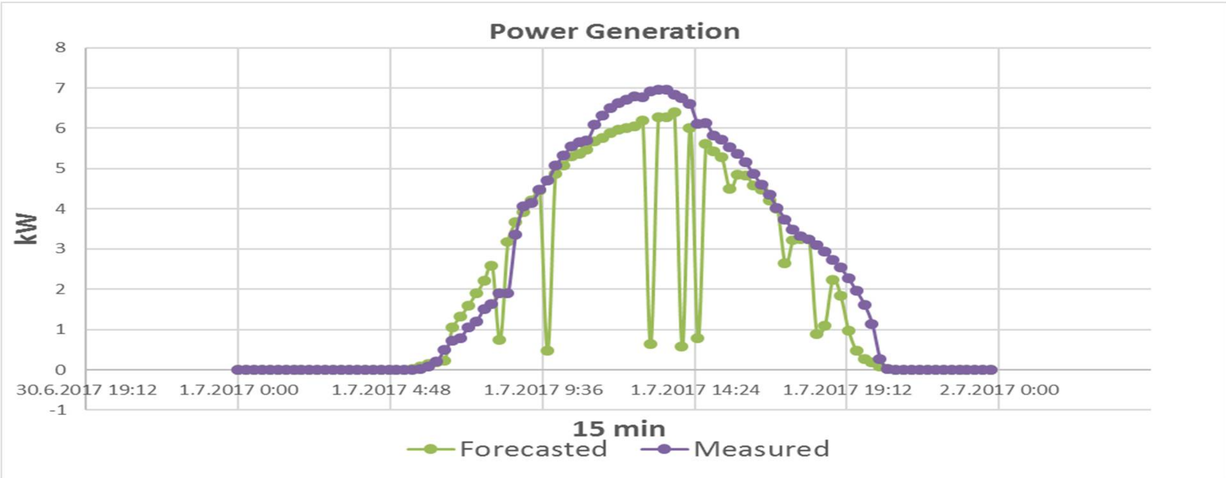

Figure 12. Photo Voltage Plant (10 kW) power generation forecast for 1 day ahead compared with measured data from Smart Meter. Violet: measured, green: forecasted

$$\mu_A(X)=\begin{cases} 0 & x \le a \\ \dfrac{x-a}{m-a} & a < x \le m \\ \dfrac{b-x}{b-m} & m < x \le b \\ 0 & x \ge b \end{cases} \tag{14}$$

$$\mu_A(X)=\begin{cases} 0 & (x < a) or (x > d) \\ \dfrac{x-a}{b-a} & a \le x \le b \\ 1 & b \le x \le c \\ \dfrac{d-x}{d-c} & c \le x \le d \end{cases} \tag{15}$$

The boundaries for MF are given in the creating and training process of FLC. Initializing of rules is performed by optimizing the rule parameters such as boundaries location and number of MFs using expert knowledge. The output boundaries from ANFIS forecasted values have huge impact on timely switching through MFs. The boundaries are defined by constant parameters of (14)-(15) and thus, it is crucial to have a valid forecasted curve. The defuzzification is done by using centroid method to cover all possible area solutions, which is defined by:

$$y = \sum_1^r \mu_j S_j \Big/ \sum_1^r \mu_j \tag{16}$$

Table 3. Parameters of the Study System.

Unit	**Value**
PV generated energy [kW]	48.80
Cb/Ecustomer,peak [kW]	48.81
$P_{peak\text{-}n}$ [kW]	5.37
P_{peak+k} [kW]	3.26
P_{peak} [kW]	5.56

Table 4. Calculated values and boundaries for FLC training according to Figure 13.

Preprints (www.preprints.org) | NOT PEER-REVIEWED | Posted: 30 September 2018 doi:10.20944/preprints201809.0594.v1

Peer-reviewed version available at *Energies* **2018**, *11*, 2953; doi:10.3390/en11112953

Unit		Data set	Value
Peak [kW]		Before	7.00
		After	5.00
Energy [kWh]		Before	337.83
		After	219.33
Generated energy [kWh]		After	59.14
Battery Bank	*SoC* [%]	After	45.15
	C_p [kWh]	After	29.62

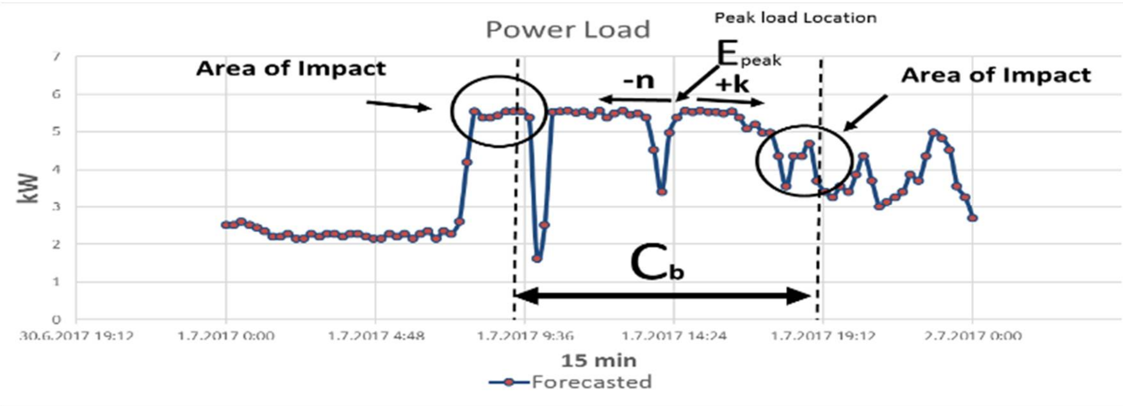

Figure 13. Designed case study for defining boundaries and Energy for load peak.

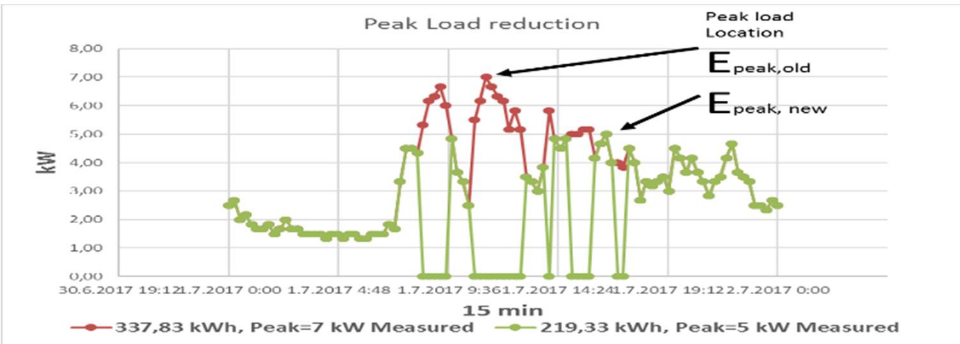

Figure 14. Obtained results from Smart Meter after applying proposed solution.

4. ANFIS Forecasting application

4.1. *Case 1: Daily Power Demand Curve*

The required data for power prediction modeling is acquired from smart meter by recording daily samples with 15-minute resolution for a three years' period. In this paper, the ANFIS forecasting system has 2 inputs and 1 output. The inputs are measured power demand from smart meter with 15-minute resolution and one daily value for temperature. For training purposes, the samples are taken for last 3 years at the same measurement place and for the same customer. In three years, the smart meter has recorded 105120 samples of power demand with 15-minutes resolution. The training and test datasets consist of 100000 and 5120 samples, respectively. The average error through 2 training epochs is around 1,39%. Three rules have been created and the defuzzification method is weighted as average based on the Sugeno type model. The training parameters of ANFIS are provided in Table 2. Figs. 10-11 shows the training results. By using the proposed ANFIS-based

Preprints (www.preprints.org) | NOT PEER-REVIEWED | Posted: 30 September 2018 doi:10.20944/preprints201809.0594.v1

Peer-reviewed version available at Energies 2018, 11, 2953; doi:10.3390/en11112953

scheme, the system output shows smaller power demand than actual measured values. So, there will be some deviation in calculating needed energy for peak load.

4.2. *Case 2: Daily PV Plant Energy Generation*

In this case, as mentioned above, the acquired data for PV generation have been gathered from smart meter between DN and PV. The ANFIS has 3 inputs and 1 output. The inputs are measured generated power from smart meter with 15-minute resolution, daily sun irradiance, and daily temperature. The output is the next day daily power demand curve. For training purposes, these samples are obtained from the last one year at same measurement place for same PV plant without changing installation configuration. In one year, the available dataset includes 35040 samples of power demand with 15-minute resolution. The inputs for training consists of 30000 samples, and 5040 samples have been used for testing. The average error through 2 training epochs is around 1,1%. The defuzzification method is weighted as average based on the Sugeno decision type. Based on the results, calculated energy amount needed for peak load is smaller than measured generated energy (Figure. 12).

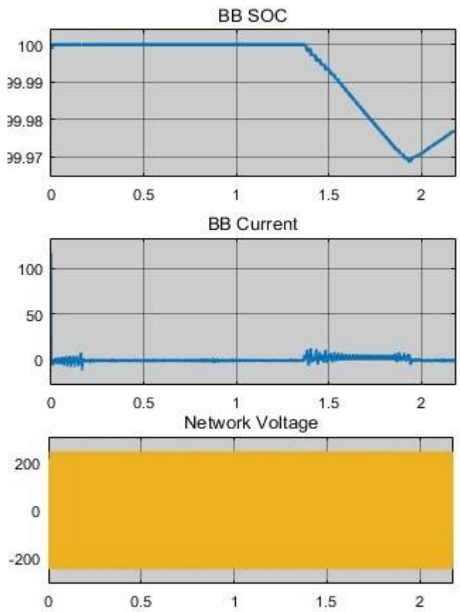

Figure 15. Current and SoC compared to DN voltage

4.3. *Fuzzy Logic Controller*

To control the switches, the IED is governed by FL-based algorithm which is trained according to the ANFIS output data. The FLC training data are obtained from load and generation, forecasted by ANFIS, the sample ordinal number from clock and the season from digital calendar. The decision type is Mamdani and based on output MF, there is a small chance for output to be uncertain in term of switching sequences 1 or 2 which result in minimal amount of space for error, not switching when needed.

Preprints (www.preprints.org) | NOT PEER-REVIEWED | Posted: 30 September 2018 doi:10.20944/preprints201809.0594.v1

Peer-reviewed version available at Energies 2018, 11, 2953; doi:10.3390/en11112953

307

308 Table 6. Inverter and PV panel technical data.

Input Data	
Inverter Model	Fronius Symo 12.5-3-M
Max. array short circuit current (MPP1 / MPP2)	40.5 A / 24.8 A
Min. input voltage ($U_{dc,min}$)	200 V
Nominal input voltage ($U_{dc,r}$)	600 V
Max. input voltage ($U_{dc,max}$)	1,000 V
MPP voltage range at P nom ($U_{mpp,\mathrm{min}}$ - $U_{mpp,max}$)	320 - 800 V
Usable MPP voltage range	200 - 800 V
Number MPP trackers	2
Number of DC connections	3 + 3
Output Data	
AC nominal output ($P_{ac,r}$)	12,500 W
Max. output power	12,500 VA
Max. output current ($I_{ac,max}$)	20 A
Min. output voltage ($U_{ac,min}$)	260 / 150 V
Max. output voltage ($U_{ac,max}$)	485 / 280 V
Frequency (f_r)	50 Hz / 60 Hz
Frequency range (f_{min} - f_{max})	45 - 65 Hz
Power factor (cos($\phi_{ac,r}$))	0 - 1 ind. / cap.
PV Panel	
Model	REC250PE-(US) BLK
STC Rating [W]	250.0
PTC Rating[W]	227.4
Open Circuit Voltage (V)	37.4
Short Circuit Current (A)	8,86
Power Tolerance	0/+5%
Weight (lbs)	39.1
Length (in)	65.55
Width (in)	39.02
Height (in)	1,50

309

Preprints (www.preprints.org) | NOT PEER-REVIEWED | Posted: 30 September 2018 doi:10.20944/preprints201809.0594.v1

Peer-reviewed version available at Energies 2018, 11, 2953; doi:10.3390/en11112953

.a) b)

.c) d)

.e) f)

Figure 18. a) PV plant on house, b) electrical cabinet and inverter, c) electrical cabinet for AC installation, d) smart meter with line breaker, e) smart UPS, and f) line breaker

Preprints (www.preprints.org) | NOT PEER-REVIEWED | Posted: 30 September 2018 doi:10.20944/preprints201809.0594.v1

Peer-reviewed version available at *Energies* **2018**, *11*, 2953; doi:10.3390/en11112953

5. Simulation results

In this section, to show the effectiveness of the proposed peak power curtailment method, the study system shown in Figure.1 (whose parameters are presented in Table 3) is modeled in MATLAB/SIMULINK environment for offline digital time-domain software simulations where different scenarios are considered. The FLC is a real-time component of the proposed solution according to operation on site and the ANFIS is conducted on measured data after the time period of one day.

5.1. Case Study

As illustrated on Figure.1, the simulated system includes three parts: PV+BESS, customer, and DN. The generation capacity of PV plant is 10 kWp, customer have minimum 10 kW power demand, and the BESS has C_P = 54 kWh. Simulation time is set to 10 sec. by steps of 0,1 sec. to simulate the system in 96 samples. When simulation starts, the sun irradiation and temperature are guiding the PV to generate electrical energy independent to BESS or DN. The BESS is set to SoC = 1% and thus, the starting point for the energy needed for peak load is equal to the forecasted amount of generated energy. A variable load is simulated and set to follow the measured load curve from Figure.9 and the boundaries are set according to Table 4. The required boundaries for FLC training are gathered by analyzing Figure.13. The data presented in Table 4 and the forecasted power demand from Figure.13 are taken to create the FLC algorithm and then it will be uploaded to IED (Figs. 1 and 13). After running simulations using real measured data, the obtained results are presented in Figure.14 and Table 4. Table 4 presents clear insight about effectiveness of the proposed method for load peak reduction. Saving in power and energy are 2 kW and 118,50 kWh, respectively. Considering the scale of the modeled study system, this is a huge saving according to leased power. Simulation started with SoC = 1% for BESS, and thereafter, PV generates almost 60 kWh, therefore the SoC of BESS after peak reduction is 45,15% namely 24,38 kWh. This brings entire model to new refreshed start position for the next day round with more capacity to count on. Figure.15 shows the steady SoC curve from BESS in the switching moment, compared to the BESS current flow and DN voltage. Based on the obtained simulation results, the BESS does not make any threat from DSO for voltage quality of the customer. This is due to passive and fast involvement of batteries into the voltage conditions of network-customer relationship. It also reveals that with right algorithm and dimensioned PV plant, the BESS can make reasonable solution to peak power curtailment problem in particular cases.

Table 5. Comparative results

Method	Time	Result	
		J_P	SoC [%]
Ref. [29]	24 hours	0.09	0.0
Ref. [30]		0.08	0.1
This paper method		0.28	45.15

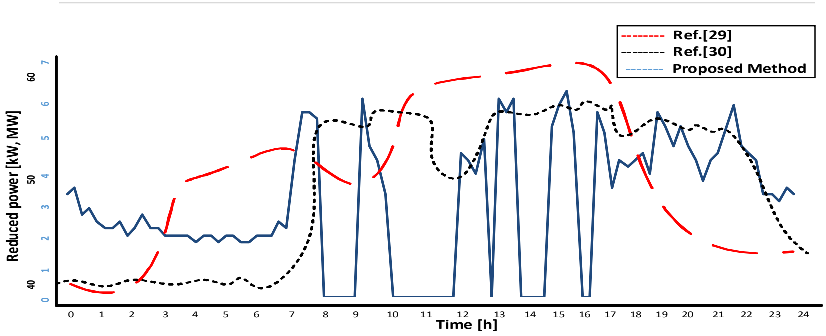

Figure 16. Aggregated results from [29]-[30] and this paper regarding Prate.

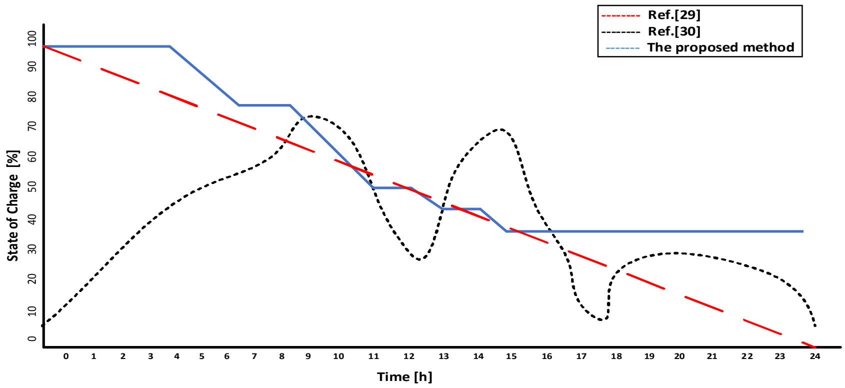

Figure17. Aggregated results from [29]-[30] and this paper regarding battery SoC.

5.2. Comparison

In this section, the simulation results for the proposed peak power curtailment method is compared with two reported techniques [29]-[30]. To have a fair comparison, all of the aggregated curves are reduced to 24 hours' time period (Figs. 21-22). The forecasted curves are not compared due to different obtained results between the proposed method and previously-reported techniques. Also, Table 5 presents the comparative results and Figs. 16-17 illustrate the comparison of all methods for the reduced power and SoC curves. When the proposed method is compared with [29]-[30], we define an index to calculate the percentage of decrement in peak power that is defined as:

$$J_P = \frac{P_{\max\_old} - P_{\max\_new}}{P_{\max\_old}} \qquad (17)$$

It can be obviously observed from the presented results that the proposed method has better performance for peak power curtailment (more than twice JP index) in contrast with the reported techniques [29]-[30]. This superiority and inherent benefit is a consequence of using different technologies in one purpose and moreover, and taking the advantage of combining of ANFIS, FL, RERs and BESS in a new hybrid configuration. However, the optimization/optimal sizing of the system components is still an interesting field of investigation for researchers [23]-[26].

6. Experimental results

The Proposed method is experimentally tested on a practical PV power plant with added BESS whose parameters are presented in Tables 5 and 6. The PV plant consists of two PV strings each have 10 panels connected with two separated maximum power point tracking (MPPT) inputs on inverters. The total number of PV panels is 40 which generates about 10kW output power. An electrical cabinet

Preprints (www.preprints.org) | NOT PEER-REVIEWED | Posted: 30 September 2018 doi:10.20944/preprints201809.0594.v1

Peer-reviewed version available at Energies 2018, 11, 2953; doi:10.3390/en11112953

is located under roof of the house visible from outside, where is the inverters are also visibly located. The smart meter between PV and DN is located near house entrance, one floor down from inverter position. In the cabinet, in addition to the smart meter, a line breaker is included that is suitable for remote control. Originally, the BESS has not been included in the installation of the PV plant. Thus, for experiment purposes, it is required to install ESS, two switches and IED. The Installation has been done between upper floor where the electrical cabinet and inverter have been installed, and down floor where the smart meter and line breaker have been included. The described disposition of components and PV plant are depicted in Figure 18.

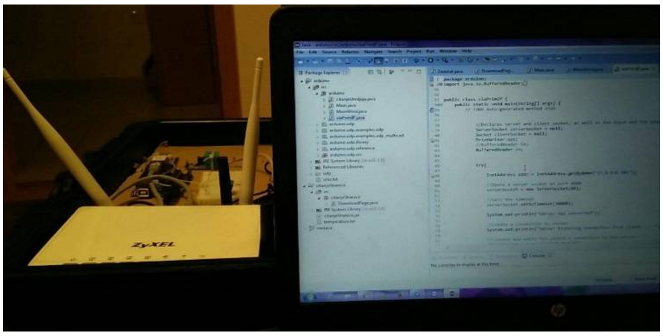

Figure 19. The IDE assembled with Arduino UNO R3 and additional components, and laboratory environment for ANFIS training and fuzzy controller design.

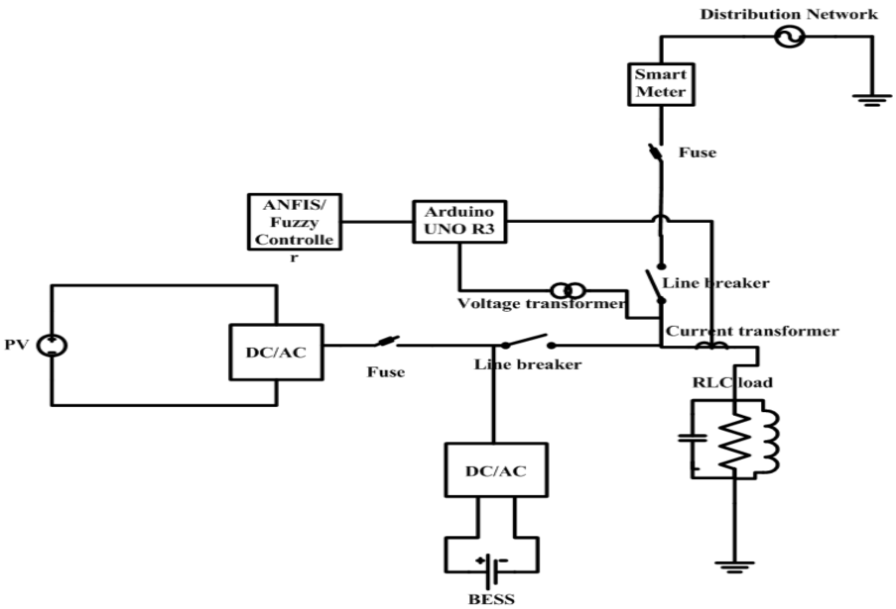

Figure 20. Single line diagram of the experiment.

Details of the additional equipment acquired and installed are as follows:

1) BESS - APC SMART Uninterruptable Power Supply (UPS) DP 1000 (used for energy storage function): with 10 kW output power (Figure.18(e)). The available UPS had already installed DC/AC inverter. So, there was no need for additional equipment regarding battery management. UPS was made in year 2004 but the batteries were not saturated due to firm housing and storing.

2) Line breakers – 2xHAGER H3 160 (used for remote switching): The mentioned line breaker is under IEC 60947-2 standard for monitoring and secondary auxiliary for control (Figure. 18(f)).

Preprints (www.preprints.org) | NOT PEER-REVIEWED | Posted: 30 September 2018 doi:10.20944/preprints201809.0594.v1

Peer-reviewed version available at *Energies* **2018**, *11*, 2953; doi:10.3390/en11112953

3) IDE (Laptop HP 250 G6): For FLC role base and ANFIS forecasting system, Arduino UNO R3, current sensor, voltage sensor, ENC28J60 network module, ZYXEL 300 mbps Wi-Fi router for data acquisition, and line breaker remote controller (Figure. 19).

For FLC design and ANFIS training, MATLAB 2017a software has been used and all decision calculations and Java programming/application has been developed in Eclipse LUNA 4.4.2. Java application, and laptop Wi-Fi has been used for listening IP address where Arduino UNO R3 was placing measured data. All mentioned components are installed according to single line diagram presented in Figure. 20.

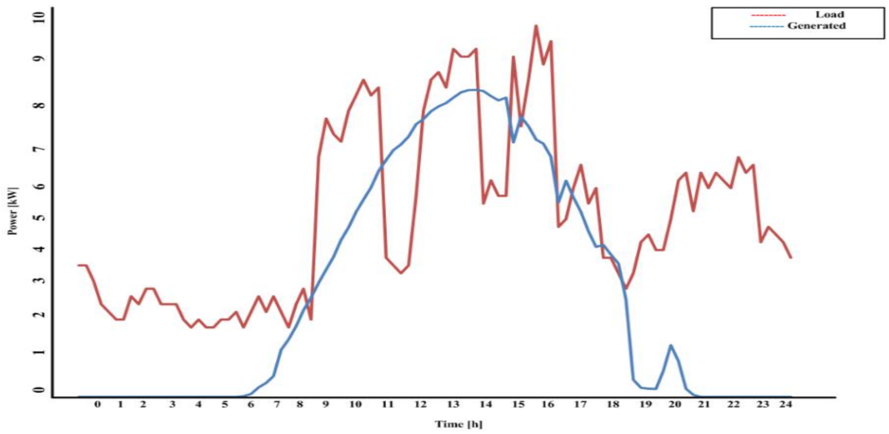

Figure 21. Forecasted daily power generation and load for experiment day.

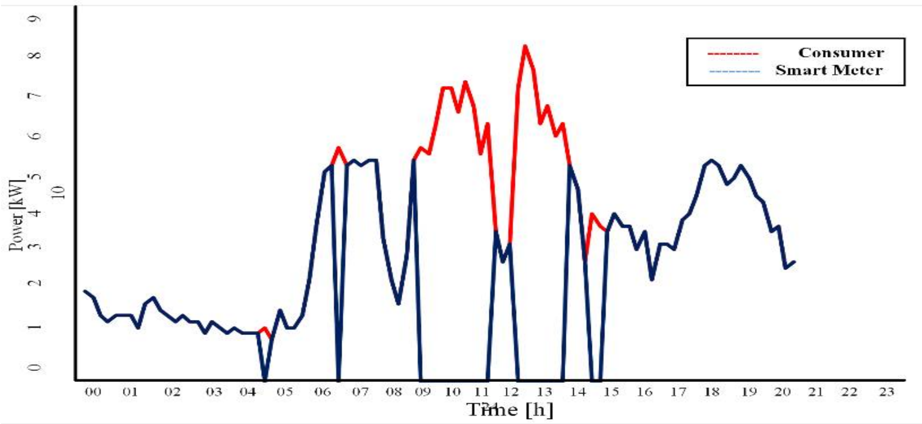

Figure 22. Experiment results recorded from smart meter and consumer measurement via Arduino Uno.

Table 7. Experiment results

Unit		Data set	Value
Peak [kW]		Consumer	9,33
		Smart Meter	6,16
Energy [kWh]		Consumer	102,33
		Smart Meter	66,00
Generated energy [kWh]		After exper.	54,42
BESS	*SoC* [%]	After exper.	100,00
	C_p [kWh]	After exper.	10,00

The experiment has been run on the date 21.08.2017. According to procedure presented in section V where is similar case study examined, all needed preparations have been done in laboratory, including parameterization of IDE (communication, Arduino-line breaker, program loading into Arduino motherboard, Wi-Fi communication setup, ANFIS-based forecasted load and PV power generation for next day, and FLC setup according to forecasted data). After laboratory work, the setup has begun on field before start of 21.08.2017, so input signals from current and voltage transformers (CT and VT) can be taken into consideration to control the line breaker. At the start of 21.08.2017, Arduino has started collecting data giving information to FLC that has been previously modelled in laptop via Wi-Fi, and gathering output data from FLC via Wi-Fi. Arduino controls line breakers according to the signals given from FLC and the proposed method is realized. The forecasted results for experiment day are illustrated in Figure 21. From Figure 21, can be clearly concluded that the generated power will not be sufficient for recharging the BESS after peak curtailment, if the BESS takes the entire energy demand on itself. So, some optimizations shall be done before conducting the experiment. For this experiment, the SOC of the BESS is 100% and the power generation should be enough for recharging part of the spent energy from BESS. The goal is to curtail the load peak, but not discharging the BESS to *SoC* = 0%. Instead, it is curtailing the peak load with equal energy to generated one. In this case, the SoC will be close to 99% at the end of day. The experimental results are provided in Table 7 and Figure. 22. It can be observed from Table 7 that the PV generated energy has completely recharged the BESS and even more energy is injected into DN. The customers' maximum power demand was under maximum battery capacity and therefore, the BESS was able to take load on itself releasing load from DN. Thus, the smart meter didn't record the load higher than 6,16 kW. There is more place for more detailed optimization of FLC for the sake of spending entire PV generated energy on consumer's load demand, instead of injecting it to DN. Anyway, the proposed method has proven to effectively manage the available stored energy for peak load curtailment in combination with PV plant.

7. Conclusion

The interest for power peak management is always popular and smart grid standards obligates the power peak curtailment. The practicality of the optimization methods for forecasting and controlling DN is rapidly growing which brings its wide area application. In this paper, we proposed a new method based on ANFIS and fuzzy logic for power peak curtailment and smart power management using DERs/RERs and BESS. Simulation results revealed that the combination of different components offer better solution. However, hybrid solutions have some limitations in form of retrain ability, specific information requirements, and expert knowledge for its maintenance. The presented model was designed to easily extend for any type of DER/RER and BESS, customer or DN. It was observed that ANFIS and FLC are flexible component and easily adaptable to any new configuration situation. Also, by analyzing results, comparing the proposed method with previously reported techniques, and performing experimental tests on a real-life practical distribution system, we conclude that the proposed method is effective and optimal for power peak curtailment.

8. Acknowledgment

Authors acknowledge support from Distribution of electric energy HZ-HB dd Mostar, in form of data acquisition.

References

[1] H.R. Baghaee, M. Mirsalim, G.B. Gharehpetian, H.A. Talebi "A new current limiting strategy and fault model to improve fault ride-through capability of inverter interfaced DERs in autonomous

microgrids", *Sustainable Energy Technologies and Assessments*, vol. 24, part C, pp. 71-81, December 2017, DOI: 10.1016/j.seta.2017.02.004.

[2] H.R. Baghaee, M. Mirsalim, G.B. Gharehpetian, H.A. Talebi, "Eigenvalue, robustness and time delay analysis of hierarchical control scheme in multi-DER microgrid to enhance small/large-signal stability using complementary loop and fuzzy logic controller", *Journal of Circuits, Systems and Computers*, vol. 26, no. 6, pp. 1-30, June 2017, DOI: 10.1142/S0218126617500992.

[3] H.R. Baghaee, M. Mirsalim, G.B. Gharehpetian, H.A. Talebi "A generalized descriptor-system robust H∞ control of autonomous microgrids to improve small and large signal stability considering communication delays and load nonlinearities", *International Journal of Electrical Power & Energy Systems*, vol. 92, no. 1, pp. 63-82, November 2017, DOI: 10.1016/j.ijepes.2017.04.007.

[4] H.R. Baghaee, M. Mirsalim, G.B. Gharehpetian, H.A. Talebi, "A Decentralized Robust Mixed H2/H∞ Voltage Control Scheme to Improve Small/Large-Signal Stability and FRT capability of Islanded Multi-DER Microgrid Considering Load Disturbances", *IEEE Systems Journal*, vol. PP, no. 99, pp. 1-12, April 2017, DOI: 10.1109/JSYST.2017.2716351.

[5] H.R. Baghaee, M. Mirsalim, G.B. Gharehpetian, H.A. Talebi "A Decentralized Power Management and Sliding Mode Control Strategy for Hybrid AC/DC Microgrids including Renewable Energy Resources", *IEEE Trans. on Industrial Informatics*, vol. PP, no. 99, pp. 1-10, March 2017, DOI: 10.1109/TII.2017.2677943.

[6] H.R. Baghaee, M. Mirsalim, G.B. Gharehpetian, H.A. Talebi, "Fuzzy Unscented Transform for Uncertainty Quantification of Correlated Wind/PV Microgrids: Possibilistic-Probabilistic Power Flow based on RBFNNs", *IET Renewable Power Generation,* in press, March 2016, pp. 1-26, March 2917, DOI: 10.1049/iet-rpg.2016.0669.

[7] H.R. Baghaee, M. Abedi, "Calculation of weighting factors of static security indices used in contingency ranking of power systems based on fuzzy logic and analytical hierarchy process", *International Journal of Electrical Power & Energy Systems*, vol. 33, no. 4, pp. 855-860, May 2011, DOI: 10.1016/j.ijepes.2010.12.012.

[8] H.R. Baghaee, M. Mirsalim, M.J. Sanjari, G.B. Gharehpetian, "Effect of type and interconnection of DG units in the fault level of distribution networks", in Proc. *13th IEEE Power Elect. & Motion Control. (EPE-PEMC)*, Poznan, Poland, Sept. 2008, pp. 313-319.

[9] Baghaee H.R., Mirsalim M., Sanjari M.J., Gharehpetian G.B., "Fault current reduction in distribution systems with distributed generation units by a new dual functional series compensator", in Proc. *13th IEEE Power Elect. & Motion Control. (EPE-PEMC)*, Poznan, Poland, PP. 1-6, September 2008.

[10] A. Karimi-Varkani, H. Monsef, H.R. Baghaee, "Strategy for participation of wind power in power market considering the uncertainty in production," *International Review of Electrical Engineering*, vol. 4, no. 5, pp. 1005-1014, September 2009.

[11] A.H. Mohsenian-Rad, V.W.S. Wong, J. Jatskevich, R. Schober, A. Leon-Garcia. "Autonomous demand-side management based on game-theoretic energy consumption scheduling for the future smart grid" *IEEE Trans. on Smart Grid*, vol. 1, no. 3, pp. 320-331, December 2010.

[12] Y. Riffonneau, S. Bacha, F. Barruel, S. Ploix. "Optimal power flow management for grid connected PV systems with batteries". *IEEE Trans. on Sustainable Energy*, vol. 2, no. 3, pp. 309-320, July 2011.

Peer-reviewed version available at Energies 2018, 11, 2953; doi:10.3390/en11112953

[13] P. Palensky, D. Dietrich. "Demand Side Management: Demand Response, Intelligent Energy Systems, and Smart Loads", *IEEE Trans. on Industrial Informatics*, vol. 7, no. 3, pp. 381-388, August 2011.

[14] K. Qian, C. Zhou, M. Allan, Y. Yuan. "Modeling of Load Demand Due to EV Battery Charging in Distribution Systems". *IEEE Trans. on Power Systems*, vol. 26, no. 2, pp. 802-810, May 2011.

[15] H.R. Baghaee, M. Mirsalim, G.B. Gharehpetian, H.A. Talebi, "Application of RBF Neural Networks and Unscented Transformation in Probabilistic Power-Flow of Microgrids including Correlated Wind/PV Units and Plug-in Hybrid Electric Vehicles", *Simulation, Modelling, Practice and Theory*, vol. 72, pp. 51-68, March 2017, DOI: 10.1016/j.simpat.2016.12.006.

[16] M.M. Siraj-Khan, M.O. Faruque,A. Newaz, "Fuzzy logic based energy storage management system for MVDC power system of all electric ship", *IEEE Trans. on Energy Conversion*, vol. 32, no. 2, pp. 798-809, June 2017.

[17] M. Hanmandlu, B.K. Chauhan. "load forecasting using hybrid models", *IEEE Trans. on Power Systems*, vol. 26, no. 1, pp. 20-29, Feb. 2011.

[18] M. Collotta, G. Pau, "An innovative approach for forecasting of energy requirements to improve a smart home management system based on BLE". *IEEE Trans. on Green Commun.. and Networking*, vol. 1, no. 1, pp. 112-120, March 2017.

[19] M.G. Simoes, B. Blunier, A. Miraoui. "Fuzzy-based energy management control: design of a battery auxiliary power unit for remote applications". *IEEE Industry Appl. Mag.*, vol. 20, no. 4, pp. 41-49, July-Aug. 2014.

[20] B. Qela, H.T. Mouftah. "Peak Load Curtailment in a Smart Grid Via Fuzzy System Approach". *IEEE Trans. on Smart Grid*, vol. 5, no. 2, pp. 761-768, March 2014.

[21] B. Bole, M.J. Daigle, G. Gorospe, "Online Prediction of Battery Discharge and Estimation of Parasitic Loads for an Electric Aircraft", Second European Conference of the Prognostics and Health Management Society 2014, Nantes, France, July 2014

[22] Y. Wang, N. Zhang, O. Chen, D.S. Kirschen, "Data-driven probabilistic net load forecasting with high penetration of behind-the-meter PV", *IEEE Trans. on Power Systems*, vol. PP, no. 99, pp. 1-10, October 2017.

[23] H.R. Baghaee, M. Mirsalim, G.B. Gharehpetian, H.A. Talebi, "Reliability/Cost based Multi-Objective Pareto Optimal Design of Stand-Alone Wind/PV/FC generation Microgrid System", *Energy*, vol. 115, part 1, no. 1, pp. 1022–1041, Nov. 2016, DOI: 10.1016/j.energy.2016.09.007.

[24] H.R. Baghaee, M. Mirsalim, G.B. Gharehpetian, A. Kashefi-Kaviani, "Security/cost-based optimal allocation of multi-type FACTS devices using multi-objective particle swarm Optimization",*Simulation: Int.Trans. Society for Modeling and Simul.*, vol. 88, no. 8, pp. 999–1010, Aug. 2012.

[25] A.K. Kaviani, H.R. Baghaee, G.H. Riahy, "Optimal sizing of a stand-alone wind/photovoltaic generation unit using particle swarm optimization", *Simulation: Int. Trans. of the Society for Modeling and Simulation*, vol. 89, no. 2, pp. 89-99, Feb. 2009, DOI: 10.1177/0037549708101181.

[26] H.R. Baghaee, M. Mirsalim, G.B. Gharehpetian, "Multi-Objective Optimal Power Management and Sizing of a Reliable Wind/PV Microgrid with Hydrogen Energy Storage using MOPSO", *J. of Intel. & Fuzzy Sys.*, vol. 32, no. 3, pp. 1753-1773, February 2017, DOI: 10.3233/JIFS-152372.

 doi:10.20944/preprints201809.0594.v1

Peer-reviewed version available at *Energies* **2018**, *11*, 2953; doi:10.3390/en11112953

[27] D. Mlakić, S. Nikolovski, D. Vucinic. "Standalone application using JAVA and ANFIS for predicting electric energy consumption based on forecasted temperature". In Proc. *27th DAAAM Int. Symp*., Viena, Austria, vol. 27, pp. 671-677, 2016.

[28] F. Grimaccia, S. Leva, M. Mussetta E. Ogliari. "ANN Sizing Procedure for the Day-Ahead Output Power Forecast of a PV Plant". *Applied Sciences,* vol. 7, no. 6, pp. 1-13, June 2017.

[29] A. Rahimi, M . Zarghami, M. Vaziri, S. Vadhva. "A simple and effective approach for peak load shaving using battery storage systems", in Proc. *North Americ. Power Symp. (NAPS)*, Manhattan, KS, USA, September 2013, pp. 1-5.

[30] C. Lu, H. Xu, X. Pan, J. Song. "Optimal Sizing and Control of Battery Energy Storage System for Peak Load Shaving", *Energies*, vol. 7, no. 12, pp. 8396-8410, December 2014.